
Multi-scale Deep Neural Networks for Solving High Dimensional PDEs*

Wei Cai

cai@smu.edu

Dept of Mathematics, Southern Methodist University
Dallas, TX 75257, United States

Zhi-Qin John Xu[†]

xuzhiqin@sjtu.edu.cn

School of Mathematical Sciences,
MOE-LSC and Institute of Natural Sciences,
Shanghai Jiao Tong University,
Shanghai, 200240, P.R. China

Abstract

In this paper, we propose the idea of radial scaling in frequency domain and activation functions with compact support to produce a multi-scale DNN (MscaledDNN), which will have the multi-scale capability in approximating high frequency and high dimensional functions and speeding up the solution of high dimensional PDEs. Numerical results on high dimensional function fitting and solutions of high dimensional PDEs, using loss functions with either Ritz energy or least squared PDE residuals, have validated the increased power of multi-scale resolution and high frequency capturing of the proposed MscaledDNN.

1 Introduction

Deep neural network (DNN) has found many application outside its traditional applications such as image classification and speech recognition into the arena of scientific computing (Han & E 2016, E et al. 2017, Khoo et al. 2017, He et al. 2018, Fan et al. 2018, Han et al. 2017, Xu et al. 2019, Huang et al. 2019), which may encounter data and solution in high dimensional spaces. The high dimensionality could come from the intrinsic physical models such as the Schrodinger equation for quantum many body systems or from the high dimensional stochastic variables due to the uncertainties in a physical systems such as those from random media material properties and manufacturing stochastic variance. DNN has been recognized as a potential tool to handle the high dimensional problems from these applications. However, to apply the commonly-used DNNs to these computational science and engineering problems, we are faced with several challenges. The most prominent issue is that the DNN normally only handles data with low frequency content well, it has been shown by a Frequency Principle (F-Principle) that many DNNs learn the low frequency content of the data quickly with good generalization error, but they will be inadequate when high frequency data are involved (Xu et al. 2018, Xu 2018, Xu et al. 2019, Rahaman et al. 2018, Zhang et al. 2019, Luo et al. 2019). As a numerical approximation technique, this behavior of DNN is quite the opposite of that of the popular multigrid methods for solving PDEs where the convergence is achieved first in the high frequency spectrum of the solution. This feature of DNN will create problem when our physical phenomena demonstrate high frequency behavior such as high frequency wave propagation

*October 24, 2019.

[†]Corresponding author

in random media or excited states of a quantum system calculated with the Schrodinger equations of many particles.

In this paper, we will propose a procedure to construct multi-scale DNNs, termed MscaleDNN, to speed up the approximation over a wide range of frequencies of high dimensional functions and apply the resulting technique for the solution of PDEs in high dimensions. The key idea is to find a way to convert the learning or approximation of high frequency data to that of a low frequency one. This approach has been attempted in a previous work in the development of a phase shift DNN (PhaseDNN) (Cai et al. 2019), where the high frequency component of the data was given a phase shift downward to a low frequency spectrum, the learning of the shifted data can be achieved with a small sized DNN quickly, which was then shifted (upward) to give approximation to the original high frequency data. The PhaseDNN has been shown to be very effective to handle highly oscillatory data from solution of high frequency Helmholtz equation and functions of small dimensions. Due to the phase shift employed along each coordinate direction, the PhaseDNN will have an intrinsic curse of dimensionality issue, therefore, can not be applied to high dimensional problems. In this study, we will propose a different method to achieve the conversion of high frequency to lower one by using a radial partition of the Fourier space and applying a scaling down operation to low frequency to learn high dimensional functions. because of the scaling operation along the radial direction in the k-space, this approach naturally avoids the curse of dimensionality issue of the PhaseDNN.

The rest of the paper is organized as follows. In section 2, we will introduce the idea of frequency scaling to generate a multi-scale DNN representation as well as that of compact supported activation function, the latter will allow the multi-scale resolution capability of the resulting DNNs. Section 3 will present two minimization approaches for finding the solution of elliptic PDEs: one through the Ritz energy, the other through least square residual error of the PDEs. Next, numerical results of high dimensional and high frequency function fitting as well as the solution of high dimensional PDEs by the proposed MscaleDNN will be given in Section 4. Finally, Section 5 gives a conclusion and some discussion for further work.

2 The idea of frequency scaled DNN and activation function with compact support

Our overall goal is to find the solution to the following high dimensional elliptic PDE,

$$-\epsilon \nabla^2 u + V(r)u = f(\mathbf{r}), \quad \mathbf{r} \in \Omega \subset R^d, d \gg 1,$$

where $\epsilon = \frac{\hbar^2}{2m}$ for Schrodinger equations, $V(\mathbf{r})$ from the external potential such as from the nucleus and external excitations.

As the solution $u(\mathbf{r})$ can be very high dimensional and we hope to find a DNN approximation to

$$T^*(\mathbf{r}, \theta) \sim u(\mathbf{r}). \quad (1)$$

In this section, we will discuss a naive idea how to use phase scaling in Fourier wave number space to reduce a high frequency learning problems to a low frequency learning for the DNN and will also point out the difficulties it may encounter as a practical algorithm.

Consider a band-limited function $f(\mathbf{r}), \mathbf{r} \in R^d$ whose Fourier transform $\hat{f}(\mathbf{k})$ has a compact support, i.e.,

$$\text{supp } \hat{f}(\mathbf{k}) \subset B(K_{\max}) = \{\mathbf{k} \in R^d, |\mathbf{k}| \leq K_{\max}\}. \quad (2)$$

We will first partition the domain $B(K_{\max})$ as union of M concentric annulus with uniform or non-uniform width, e.g.,

$$A_i = \{\mathbf{k} \in R^d, (i-1)K_0 \leq |\mathbf{k}| \leq iK_0\}, K_0 = K_{\max}/M, 1 \leq i \leq M \quad (3)$$

so that

$$B(K_{\max}) = \bigcup_{i=1}^M A_i. \quad (4)$$

Now, we can decompose the function $\widehat{f}(\mathbf{k})$ as follows

$$\widehat{f}(\mathbf{k}) = \sum_{i=1}^M \chi_{A_i}(\mathbf{k}) \widehat{f}(\mathbf{k}) \triangleq \sum_{i=1}^M \widehat{f}_i(\mathbf{k}), \quad (5)$$

where

$$\sup \widehat{f}_i(\mathbf{k}) \subset A_i. \quad (6)$$

The decomposition in the k -space give a corresponding one in the physical space

$$f(\mathbf{r}) = \sum_{i=1}^M f_i(\mathbf{r}), \quad (7)$$

where

$$f_i(\mathbf{r}) = \mathcal{F}^{-1}[\widehat{f}_i(\mathbf{k})](\mathbf{r}) = f(\mathbf{r}) * \chi_{A_i}^\vee(\mathbf{r}), \quad (8)$$

and the inverse Fourier transform of $\chi_{A_i}(\mathbf{k})$ is called the frequency selection kernel (Cai et al. 2019) and can be computed analytically using Bessel functions

$$\chi_{A_i}^\vee(\mathbf{r}) = \frac{1}{(2\pi)^{d/2}} \int_{A_i} e^{i\mathbf{k} \cdot \mathbf{r}} d\mathbf{r}. \quad (9)$$

From (6), we can apply a simple down-scaling to convert the high frequency region A_i to a low frequency region. Namely, we define a scaled version of $\widehat{f}_i(\mathbf{k})$ as

$$\widehat{f}_i^{(\text{scale})}(\mathbf{k}) = \widehat{f}_i(\alpha_i \mathbf{k}), \alpha_i > 1, \quad (10)$$

and

$$f_i^{(\text{scale})}(\mathbf{r}) = f_i\left(\frac{1}{\alpha_i} \mathbf{r}\right), \quad (11)$$

or

$$f_i(\mathbf{r}) = f_i^{(\text{scale})}(\alpha_i \mathbf{r}), \quad (12)$$

noting the low frequency spectrum of the scaled function if α_i is chosen large enough, i.e.,

$$\sup \widehat{f}_i^{(\text{scale})}(\mathbf{k}) \subset \{\mathbf{k} \in \mathbb{R}^d, \frac{(i-1)K_0}{\alpha_i} \leq |\mathbf{k}| \leq \frac{iK_0}{\alpha_i}\}. \quad (13)$$

Using the F-Principle of common DNNs (Xu et al. 2019), with iK_0/α_i being small, we can train a DNN $h_i(\mathbf{r}, \theta^{n_i})$ to learn $f_i^{(\text{scale})}(\mathbf{r})$ quickly

$$f_i^{(\text{scale})}(\mathbf{r}) \sim h_i(\mathbf{r}, \theta^{n_i}), \quad (14)$$

which gives an approximation to $f_i(\mathbf{r})$ immediately

$$f_i(\mathbf{r}) \sim h_i(\alpha_i \mathbf{r}, \theta^{n_i}) \quad (15)$$

and to $f(\mathbf{r})$ as well

$$f(\mathbf{r}) \sim \sum_{i=1}^M h_i(\alpha_i \mathbf{r}, \theta^{n_i}). \quad (16)$$

The difficulty of the above procedure for approximating function in high dimension is the need to compute the d -dimensional convolution in (8), which leads to the issue of the curse of dimensionality.

Compact supported activation function. In order to produce scale separation and identification capability of the MscaleDNN, we take the hint from the theory of compact mother scaling function in the wavelet theory (Daubechies 1992) and consider the activation functions with a compact support. This way if the activation function is scaled by a factor α , the scaled activation function will have frequency spectrum as α times that of that of the original activation function, allowing the corresponding neuron in the MscaleDNN to learn more easily the corresponding frequency of the solution.

The support of the common activation function $\text{ReLU}(x) = \max(0, x)$ is not compact. To produce an activation function with compact support, we simply use the following modified activation function.

$$\text{sReLU}(x) = \text{ReLU}(-(x - 1)) \times \text{ReLU}(x).$$

The support of sReLU is on $[0, 1]$. In order to have a differentiable activation function, we can use $(\text{sReLU}(x))^2$ and $(\text{sReLU}(x))^3$ to have continuous first and second derivatives, respectively, which are shown in Fig. 1.

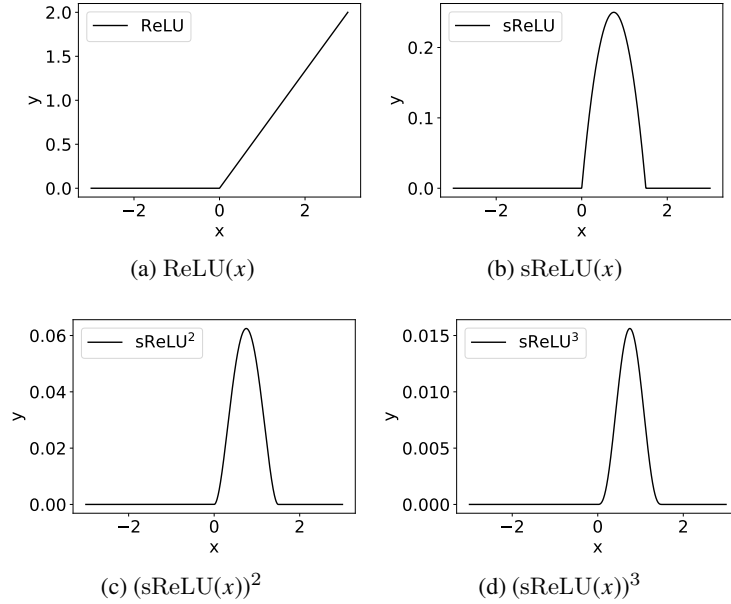


Figure 1

The weights in the MscaleDNN neurons are initialized by a normal distribution, namely, the weights are sampled from $\mathcal{D}_1 = \mathcal{N}(0, (2/(n_{\text{in}} + n_{\text{out}}))^2)$ or $\mathcal{D}_2 = \mathcal{N}(0, 2/(n_{\text{in}} + n_{\text{out}}))$, where n_{in} and n_{out} are the input and output dimensions of the corresponding layer, respectively. Note that these two initialization methods are widely used and studied (Glorot & Bengio 2010, Jacot et al. 2018, Rotskoff & Vanden-Eijnden 2018). The DNNs are trained by Adam (Kingma & Ba 2014).

3 MscaleDNN with compact supported activation function

Even though the procedure leading to (16) is not practical for high dimensional approximation, however it does suggest a plausible form of function space for finding the solution more quickly with DNN functions. We can use a series of α_i ranging from 1 to a large number to produce a MscaleDNN, which can achieve our goal to speed up the convergence for solution with many frequencies with better accuracy.

MscaleDNN structure. To realize the MscaleDNN, we separate the neuron in the first hidden-layer into to A parts. The neuron in the i -th part receives input $i\mathbf{x}$, that is, its output is $\sigma(i\mathbf{w} \cdot \mathbf{x} + b)$, where \mathbf{w} , \mathbf{x} , b are weight, input and bias term, respectively. The complete MscaleDNNs reads as

$$h(\mathbf{x}) = \mathbf{W}_L \sigma \circ (\mathbf{W}_{L-1} \sigma \circ (\cdots \sigma \circ (\mathbf{W}_1 \sigma \circ (\mathbf{K} \odot \mathbf{W}_0 \mathbf{x} + \mathbf{b}_0) + \mathbf{b}_1) \cdots) + \mathbf{b}_{L-1}) \quad (17)$$

where $\mathbf{x} \in \mathbb{R}^d$, $\mathbf{W}_l \in \mathbb{R}^{n_{l+1} \times n_l}$, n_l is the neuron number of l -th hidden layer, $n_0 = d$, $b_l \in \mathbb{R}^{l+1}$, σ is a scalar function and “ \circ ” means entry-wise operation, \odot is the Hadamard product and

$$\mathbf{K} = (\underbrace{1, 1, \cdots, 1}_{1\text{st part}}, \underbrace{2, \cdots, i-1, i, i, \cdots, i, i+1, \cdots}_{i\text{th part}}, \underbrace{A, A, \cdots, A}_{A\text{th part}})^T. \quad (18)$$

Fig. 2 shows a toy example of $A = 3$. The only difference compared with a normal fully-connected network is the input to the first hidden layer.

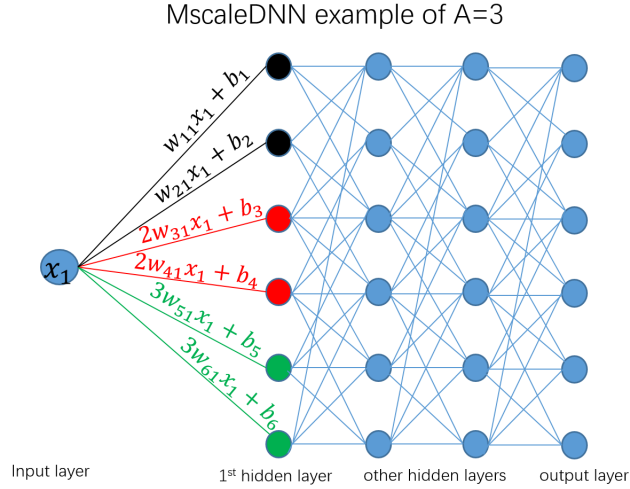


Figure 2: Illustration of a MscaleDNN.

We would use MscaleDNN to fit high-dimensional functions and high-frequency functions. We will also introduce two loss functions of using MscaleDNN for finding the solution of PDEs. We consider the following problem,

$$-\Delta u(\mathbf{x}) = g(\mathbf{x}), \quad \mathbf{x} \in \Omega, \quad (19)$$

with the boundary condition

$$u(\mathbf{x}) = \tilde{g}(\mathbf{x}), \quad \mathbf{x} \in \partial\Omega. \quad (20)$$

where $\mathbf{x} = (x_1, x_2, \cdots, x_d)$. We denote the true solution as $u_{\text{true}}(\mathbf{x})$. In each training step, we sample n points in Ω and \tilde{n} points at each hyperplane that composes $\partial\Omega$. The first loss function is based on the variational Ritz formulation of the elliptic problem and the second one is based on the mean square of the residual of the differential equation.

3.1 A Ritz variational method for PDE

The deep Ritz method as proposed by E & Yu (2018) produces a variational solution $u(\mathbf{r})$ through the following minimization problem

$$u = \arg \min_{v \in \Pi} J(v), \quad (21)$$

where the energy functional is defined as

$$J(v) = \int_{\Omega} \left(\frac{1}{2} \epsilon(\mathbf{r}) |\nabla v|^2 + V(r) v^2 \right) dr - \int_{\Omega} f(\mathbf{r}) v(\mathbf{r}) dr \triangleq \int_{\Omega} E(\mathbf{v}(\mathbf{r})) d\mathbf{r}. \quad (22)$$

We use MscaleDNN output $h(x, \theta)$ to parameterize v in the above problem, where θ is the DNN parameter set. Then, the MscaleDNN solution is

$$\theta_* = \arg \min_{\theta} J(h(x, \theta)), \quad (23)$$

The minimizer θ_* can be found by stochastic gradient decent (SGD) as in E & Yu (2018),

$$\theta^{(n+1)} = \theta^{(n)} + \eta \nabla_{\theta} J(h(x, \theta)). \quad (24)$$

The integral in Eq. (22) can not be integrated due to high dimensional curse, and in fact, will only be sampled at some random points at each training step (see (2.11) in E & Yu (2018)), that is,

$$\nabla_{\theta} J(h(x, \theta)) \sim \nabla_{\theta} \frac{1}{N_s} \sum_{s=1}^{N_s} E(h(\mathbf{r}_s, \theta)). \quad (25)$$

At convergence $\theta^{(n)} \rightarrow \theta_*$, we obtain a MscaleDNN solution $h(x, \theta_*)$ for the given material constant $\epsilon^{(s)}$.

In our numerical test of this paper, the Ritz loss function is chosen to be

$$L_{\text{ritz}}(h) = \frac{1}{n} \sum_{\mathbf{x} \in S} (|\nabla h(\mathbf{x})|^2 / 2 - g(\mathbf{x}) h(\mathbf{x})) + \beta * \frac{1}{\tilde{n}} \sum_{\mathbf{x} \in \tilde{S}} (h(\mathbf{x}) - \tilde{g}(\mathbf{x}))^2. \quad (26)$$

where $h(\mathbf{x})$ is the DNN output, S is the sample set from Ω and n is the sample size. \tilde{n} indicates sample set from $\partial\Omega$. The second penalty term is to enforce the boundary condition.

3.2 MscaleDNN least square error method for PDEs

In an alternative approach, we can simply use the loss function of Least Squared Residual Error (LSE),

$$L_{\text{LSE}}(h) = \frac{1}{n} \sum_{\mathbf{x} \in S} (\Delta h(\mathbf{x}) + g(\mathbf{x}))^2 + \beta * \frac{1}{\tilde{n}} \sum_{\mathbf{x} \in \tilde{S}} (h(\mathbf{x}) - \tilde{g}(\mathbf{x}))^2. \quad (27)$$

To see the learning accuracy, we also compute the distance between $h(\mathbf{x})$ and u_{true} ,

$$\text{MSE}(h(\mathbf{x}), u_{\text{true}}(\mathbf{x})) = \frac{1}{n + \tilde{n}} \sum_{\mathbf{x} \in S \cup \tilde{S}} (h(\mathbf{x}) - u_{\text{true}}(\mathbf{x}))^2 \quad (28)$$

4 Numerical experiments

In the following, we use solid line to indicate the train loss and dashed line to indicate the test loss. The curve of the training loss often overlaps well with that of the test loss for most cases, indicating that the neural networks generalize well.

We explain the legends in figures here. “ms1”, “ms10” and “ms100” indicate the scale number A of 1, 10 and 100, respectively. “ReLU” and “sReLU” indicate the activation functions. “train” and “test” indicate the training loss and the test loss, respectively. All networks are trained by Adam (Kingma & Ba 2014).

4.1 Fitting 3-dimensional functions

In this section, we use a 3d function to show that MscaleDNN can learn target function much faster than the normal one-scale network. In addition, we also show the DNN with compact-supported activation function learns faster than that of normal non-compact-supported activation function. We use DNNs to fit a 3d oscillatory function: $\mathbb{R}^3 \rightarrow \mathbb{R}$, that is,

$$f(\mathbf{x}) = \sum_{j=1}^3 \cos(10x_j) + \sin(5x_j), \quad x_j \in [-\pi/2, \pi/2], \quad (29)$$

where $\mathbf{x} = (x_1, x_2, x_3)$.

From the experiment of one-hidden layer network initialized by \mathcal{D}_1 in Fig. 3 and the multiple hidden-layer network initialized by \mathcal{D}_2 in Fig. 4, we can observe the following behaviors. First, the DNN with activation function sReLU learns much faster than that with ReLU. Second, sReLU-DNN with 100 scales is much faster than that with only 1 scale.

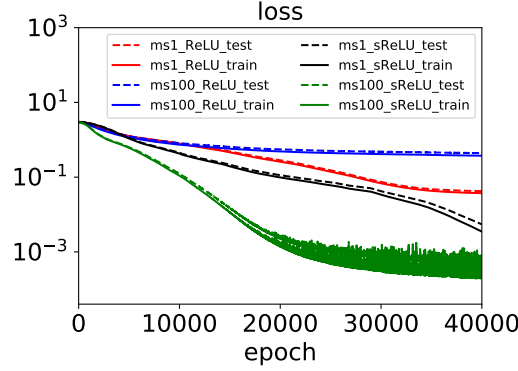


Figure 3: Loss function vs. training epoch. We use a network 3-2500-1 with activation function $\text{ReLU}(x)$ or $\text{sReLU}(x)$ indicated by the legend. The learning rate is 5×10^{-5} with a decay rate 2×10^{-7} for each full-batch training step. The training and test dataset are both 10000 random samples. Weights are initialized by \mathcal{D}_1 .

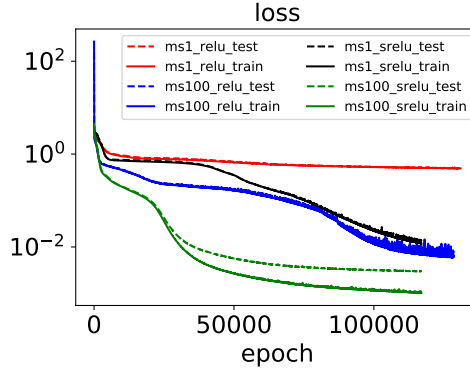


Figure 4: Loss function vs. training epoch. We use a network 3-500-500-500-500-1 with activation function $\text{ReLU}(x)$ or $\text{sReLU}(x)$ indicated by the legend. The learning rate is 3×10^{-6} with a decay rate 5×10^{-7} for each training step with batch size 1000. The training and test dataset are both 5000 random samples. Weights are initialized by \mathcal{D}_2 .

4.2 Fitting 60-dimensional functions with intrinsic low dimensional structure

Real data are often high-dimensional, however, its intrinsic dimension is often low. In this subsection, we use DNNs to fit 60-dimensional data, which has a intrinsic dimension 3. Consider

$$f(\mathbf{x}(t)) = \sum_{j=1}^{d_{in}} \cos(10t_j) + \sin(5t_j), \quad t_j \in [0, 1], \quad (30)$$

where $\mathbf{x} = (x_1, x_2, \dots, x_d)$, $\mathbf{x} = (x_1, x_2, \dots, x_d)$, $d_{in} = 3$ and $d = 60$. We use a DNN of d-200-200-200-1. We would consider a linear embedding and a non-linear embedding situation.

For the linear embedding example, we consider

$$x_i = \cos(i)t_{\lfloor i/(d/d_{in}) \rfloor}, \quad (31)$$

where $\lfloor \cdot \rfloor$ is the operation of taking the integer part.

For the non-linear embedding example, we consider,

$$x_i = \cos(\cos(i)t_{\lfloor i/(d/d_{in}) \rfloor}). \quad (32)$$

For the networks initialized by \mathcal{D}_1 , as shown by the training loss functions in Fig. 5 (a, b), the MscaledDNN with sReLU is faster in learning both linear and nonlinear embedded data. Note that the MscaledDNN with ReLU does not show advantage with more scales, as shown in Fig. 5 (c). For the networks initialized by \mathcal{D}_2 , as shown in Fig. 6, results are similar.

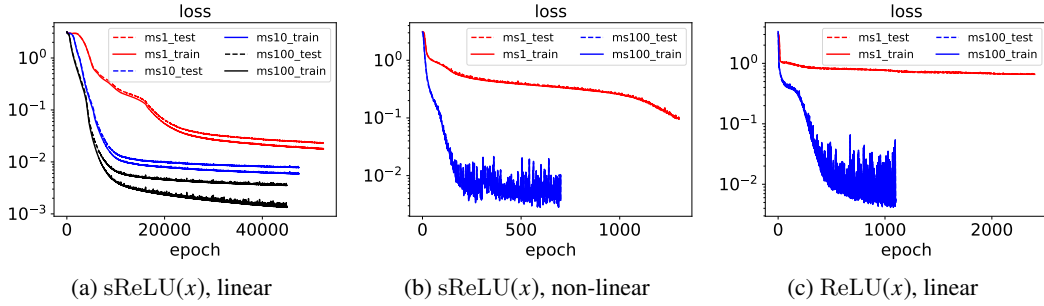


Figure 5: Loss function vs. training epoch. We use a network 60-200-200-200-1 with activation function sReLU(x) or ReLU(x). The learning rate is 5×10^{-5} with a decay rate 2×10^{-7} for each training step with batch size 100. The training and test dataset are both 10000 random samples. Weights are initialized by \mathcal{D}_1 .

4.3 Fitting high-frequency function

Approximating high-frequency functions are very important in physical problems. In this section, we use DNNs to fit high-frequency functions for 1d and 2d problems with MSE loss function.

1d problems. Consider

$$f(x) = \sin(23x) + \sin(137x) + \sin(203x), \quad x \in [0, \pi].$$

As shown in Fig. 7, with only one-scale DNN, the loss function decreases very slow during the training, while the loss function of the MscaledDNN decrease rapidly. We visualize the learned curves on test data points in Fig. 8. For the one-scale DNN (first row in Fig. 8), the DNN learns a low-frequency function which cannot capture the target function. On the contrary, the MscaledDNN (second row in Fig. 8) accurately captures the highly oscillation of the target function.

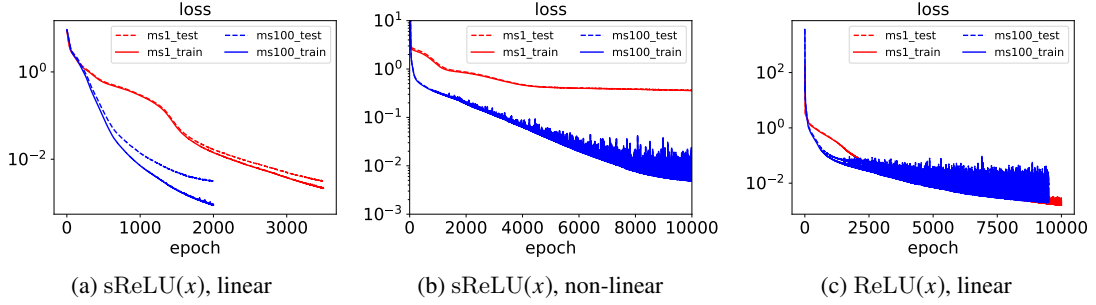


Figure 6: Loss function vs. training epoch. We use a network 60-500-500-500-500-1 with activation function sReLU(x) or ReLU(x). The learning rate is 10^{-5} with a decay rate 5×10^{-7} for each training step with batch size 1000. For the non-linear embedding example in (b), we use a smaller learning rate to avoid the fluctuation of loss function, 3×10^{-6} . The training and test dataset are both 5000 random samples. Weights are initialized by \mathcal{D}_2 .

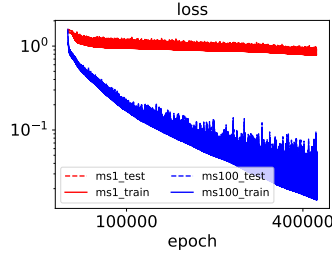


Figure 7: Loss function vs. training epoch. Fitting high-frequency 1d function. We use a network 1-1000-500-500-500-500-1 with activation function sReLU(x). The learning rate is 10^{-5} with a decay rate 5×10^{-7} for each training step with batch size 1000. The training and test dataset for 1d are 5000 and 1000 random samples, respectively. Weights are initialized by \mathcal{D}_2 .

2d problems. Consider

$$f(x, y) = f_1(x)f_1(y),$$

where

$$f_1(x) = \sin(23x) + \sin(32x), \quad x \in [0, \pi].$$

As shown in Fig. 9, similarly, the loss functions of MscaleDNN decays much faster than that of one-scale DNN during the training. On the test data points, Fig. 10 shows that the MscaleDNN predicts the target function well while one-scale DNN can not. To visualize the MscaleDNN can well predict the oscillation of the target function, we plot the true function and the DNN output at $y = 0.5$ on test data points, as shown in Fig. 10. The common one-scale DNN only captures the low-frequency oscillation, while the MscaleDNN captures well the highly oscillation of the target function.

4.4 Solving high dimensional PDE

An important application of MscaleDNN is to solve high-dimensional PDEs, which is often very difficult for traditional methods due to the curse of dimensionality. A previous work (Xu et al. 2019) proposes to use DNNs to capture the low-frequency part of the solution and then use the DNN output

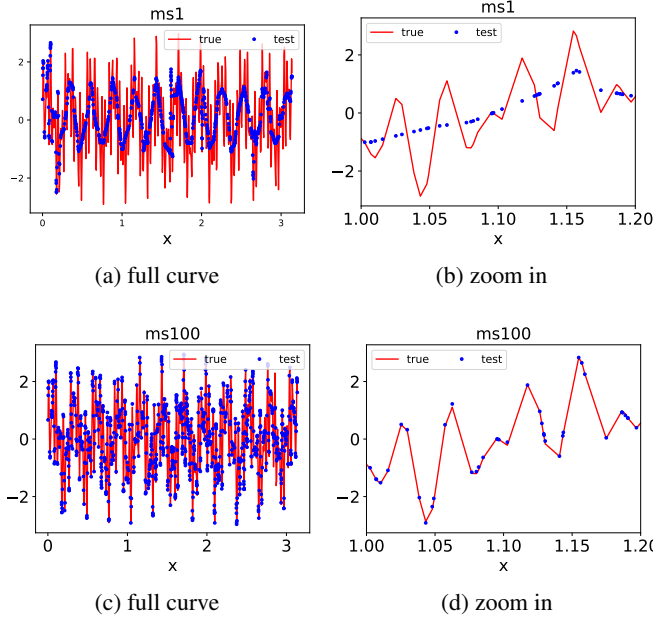


Figure 8: The learning curves in fitting high-frequency 1d function on test data points.

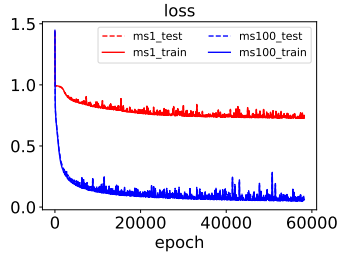


Figure 9: Loss function vs. training epoch. Fitting high-frequency 2d function. We use a network 2-1000-500-500-500-500-1 with activation function $\text{sReLU}(x)$. The learning rate is 10^{-5} and 2×10^{-5} for 1d and 2d, respectively, with a decay rate 5×10^{-7} for each training step with batch size 10000. The training and test dataset are 100000 and 50000 random samples, respectively. Weights are initialized by \mathcal{D}_2 .

after training as the initial value for traditional methods to continuously learn the high-frequency part. Later, another work (Huang et al. 2019) shows that by using DNN output as initialization for traditional methods can accelerate the solving process of many PDEs. The PhaseDNN attempts to overcome the difficulty of learning high frequency by shifting high frequency to low frequency in each coordinate. However, all these methods suffer from the curse of dimensionality. The Deep Ritz method proposed to solve PDEs with DNNs in E et al. (2017) may overcome the curse of dimensionality, however, they are not able to handle high-frequency functions efficiently due to the F-Principle behavior of traditional DNNs. The MscaleDNN uses multiple scales to facilitate the learning of many frequencies while having the potential to overcome the curse of dimensionality.

We consider the following example,

$$g(\mathbf{x}) = \sum_{i=1}^d \sin(x_i) + 100 \sin(10x_i) \quad (33)$$

and

$$\tilde{g}(\mathbf{x}) = \sum_{i=1}^d \sin(x_i) + \sin(10x_i), \quad \mathbf{x} \in \partial\Omega \quad (34)$$

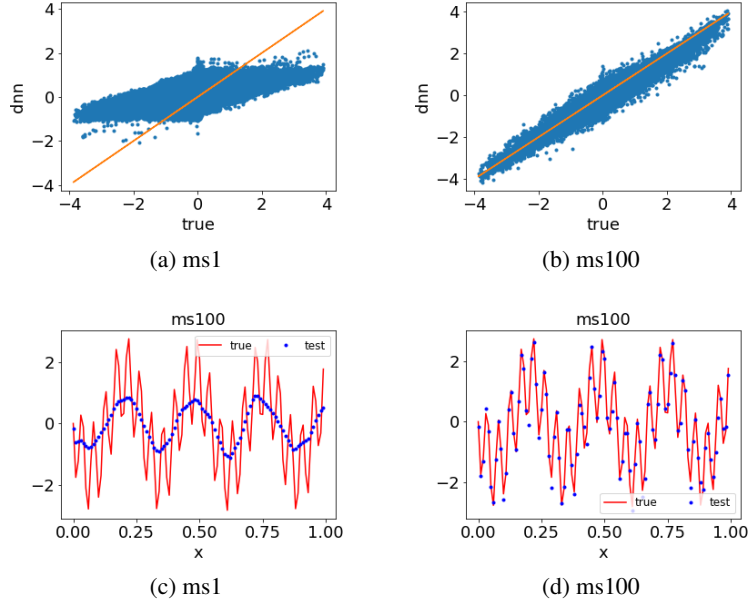


Figure 10: The learning curves in fitting high-frequency 2d function. First row: Each point corresponds to a test data point, the abscissa is the true value and the ordinate is the DNN output. Second row: The line of $y = 0.5$ for the true function and the DNN output at test data points.

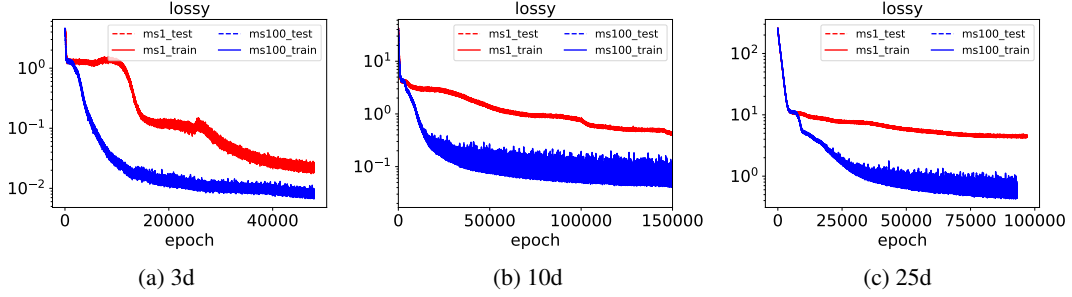


Figure 11: Ritz loss: $\text{MSE}(h(\mathbf{x}), u_{\text{true}}(\mathbf{x}))$ vs. training epoch. sReLU(x). Ritz loss. $\Omega = [0, 1]^d$, $n = 1000$, $\tilde{n} = 100$, $\beta = 1000$, we use a network d-200-200-200-1 with activation function sReLU(x). The learning rate is 5×10^{-5} with a decay rate 5×10^{-7} for each training step. Weights are initialized by \mathcal{D}_1 .

The true solution is

$$u_{\text{true}}(\mathbf{x}) = \sum_{i=1}^d \sin(x_i) + \sin(10x_i). \quad (35)$$

Results with both Ritz loss in Eq. (26) and LSE loss in Eq. (27) are given below.

Ritz loss We show $\text{MSE}(h(\mathbf{x}), u_{\text{true}}(\mathbf{x}))$ during the training process for $d = 3, 10, 25$ in Fig. 11 with initialization \mathcal{D}_1 and in Fig. 12 with initialization \mathcal{D}_2 . In all cases, MscaleDNNs with 100 scales are much faster than that of only one scale. Note that if we only use the activation function of $\sigma(100\mathbf{w} \cdot \mathbf{x} + b)$ for the first hidden layer, the learning is very slow.

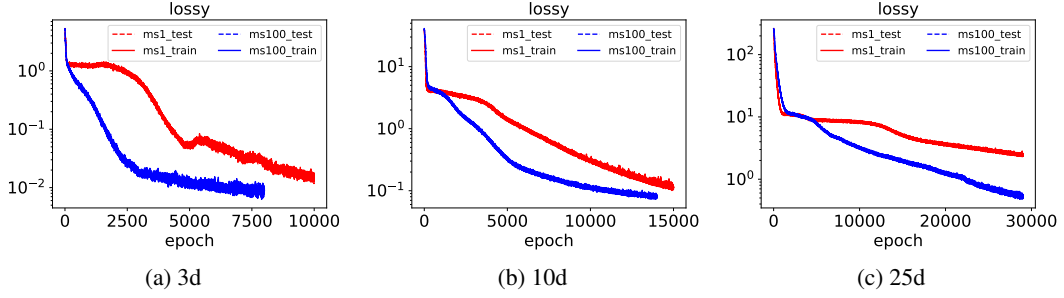


Figure 12: Ritz loss: $\text{MSE}(h(\mathbf{x}), u_{\text{true}}(\mathbf{x}))$ vs. training epoch. sReLU(x). Ritz loss. $\Omega = [0, 1]^d$, $n = 1000$, $\tilde{n} = 100$, $\beta = 1000$, we use a network d-500-500-500-1 with activation function sReLU(x). The learning rate is 5×10^{-5} with a decay rate 5×10^{-7} for each training step. Weights are initialized by \mathcal{D}_2 .

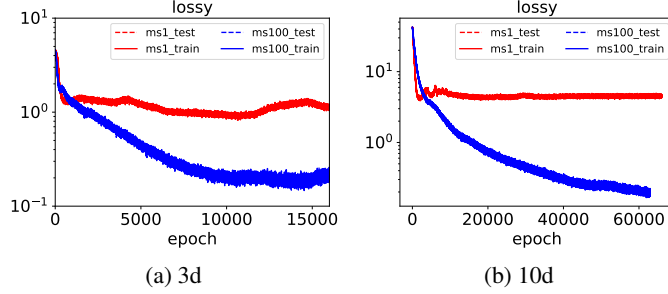


Figure 13: LSE loss: $\text{MSE}(h(\mathbf{x}), u_{\text{true}}(\mathbf{x}))$ vs. training epoch. Direct loss. $\Omega = [0, 1]^d$, $n = 1000$, $\tilde{n} = 100$, $\beta = 1000$, we use a network d-200-200-200-1 with activation function sReLU(x). The learning rate is 5×10^{-5} with a decay rate 5×10^{-7} for each training step. Weights are initialized by \mathcal{D}_1 .

LSE loss We show $\text{MSE}(h(\mathbf{x}), u_{\text{true}}(\mathbf{x}))$ during the training process for $d = 3, 10$ in Fig. 13 with initialization \mathcal{D}_1 and in Fig. 14 with initialization \mathcal{D}_2 . In all cases, MscaleDNNs with 100 scales are much faster than that of only one scale. Note that since the LSE loss requires Laplacian operation, its computational cost is much higher.

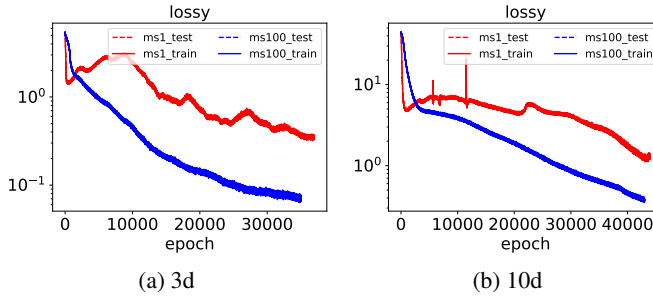


Figure 14: LSE loss: $\text{MSE}(h(\mathbf{x}), u_{\text{true}}(\mathbf{x}))$ vs. training epoch. Direct loss. $\Omega = [0, 1]^d$, $n = 5000$, $\tilde{n} = 100$, $\beta = 1000$, we use a network d-200-200-200-1 with activation function sReLU(x). The learning rate is 5×10^{-5} with a decay rate 5×10^{-7} for each training step. Weights are initialized by \mathcal{D}_2 .

5 Conclusion and future work

In this paper, we have introduced a frequency domain scaling DNN with compact supported activation function, MscaleDNN, to produce a multi-scale DNN for approximating function of high frequency and high dimensions as well as the solution of PDEs in high dimensions. By using the radial scaling in the k -space of the functions, we are able to achieve much faster learning results for high dimensional function fitting and solution of elliptic problems though either least square residual or Ritz energy minimization. While the Ritz minimization approach only requires the first derivatives of the DNN solution, the least square residual, which does need to compute the full Laplacian of the DNN, thus incurring a higher cost, can be applicable to non-self adjoint differential operators, such as high dimensional Fokker-Planck equations.

In the current implementation of MscaleDNN, we only used neurons with scaled compact supported activation functions, this corresponds to the scaling spaces in the wavelet theory. Because many scales are used in the first hidden layer of the MscaleDNN, we actually created much redundancy or overlapping of scales in the neurons. A more sophisticated way, following the idea of mother wavelet function (Daubechies 1992), is to introduce another type of neuron made of activation function with similar properties of the mother wavelet, such as vanishing moments, leading to a Wavelet-DNN multi-resolution framework for high dimensional problem.

6 Acknowledgments

The second author is supported by the Student Innovation Center at Shanghai Jiao Tong University and thanks Douglas Zhou (SJTU) for providing computational resource.

References

- Cai, W., Li, X. & Liu, L. (2019), ‘A phase shift deep neural network for high frequency wave equations in inhomogeneous media’, *Arxiv preprint, arXiv:1909.11759*.
- Daubechies, I. (1992), *Ten lectures on wavelets*, Vol. 61, Siam.
- E, W., Han, J. & Jentzen, A. (2017), ‘Deep learning-based numerical methods for high-dimensional parabolic partial differential equations and backward stochastic differential equations’, *Communications in Mathematics and Statistics* **5**(4), 349–380.
- E, W. & Yu, B. (2018), ‘The deep ritz method: A deep learning-based numerical algorithm for solving variational problems’, *Communications in Mathematics and Statistics* **6**(1), 1–12.
- Fan, Y., Lin, L., Ying, L. & Zepeda-Núñez, L. (2018), ‘A multiscale neural network based on hierarchical matrices’, *arXiv preprint arXiv:1807.01883*.
- Glorot, X. & Bengio, Y. (2010), Understanding the difficulty of training deep feedforward neural networks, in ‘Proceedings of the thirteenth international conference on artificial intelligence and statistics’, pp. 249–256.
- Han, J. & E, W. (2016), ‘Deep learning approximation for stochastic control problems’, *arXiv:1611.07422*.
- Han, J., Zhang, L., Car, R. et al. (2017), ‘Deep potential: A general representation of a many-body potential energy surface’, *arXiv preprint arXiv:1707.01478*.
- He, J., Li, L., Xu, J. & Zheng, C. (2018), ‘Relu deep neural networks and linear finite elements’, *arXiv preprint arXiv:1807.03973*.
- Huang, J., Wang, H. & Yang, H. (2019), ‘Int-deep: A deep learning initialized iterative method for nonlinear problems’, *arXiv preprint arXiv:1910.01594*.

- Jacot, A., Gabriel, F. & Hongler, C. (2018), Neural tangent kernel: Convergence and generalization in neural networks, *in* ‘Advances in neural information processing systems’, pp. 8571–8580.
- Khoo, Y., Lu, J. & Ying, L. (2017), ‘Solving parametric pde problems with artificial neural networks’, *arXiv preprint arXiv:1707.03351* .
- Kingma, D. P. & Ba, J. (2014), ‘Adam: A method for stochastic optimization’, *arXiv preprint arXiv:1412.6980* .
- Luo, T., Ma, Z., Xu, Z.-Q. J. & Zhang, Y. (2019), ‘Theory of the frequency principle for general deep neural networks’, *arXiv preprint arXiv:1906.09235* .
- Rahaman, N., Arpit, D., Baratin, A., Draxler, F., Lin, M., Hamprecht, F. A., Bengio, Y. & Courville, A. (2018), ‘On the spectral bias of deep neural networks’, *arXiv preprint arXiv:1806.08734* .
- Rotskoff, G. & Vanden-Eijnden, E. (2018), Parameters as interacting particles: long time convergence and asymptotic error scaling of neural networks, *in* ‘Advances in neural information processing systems’, pp. 7146–7155.
- Xu, Z. J. (2018), ‘Understanding training and generalization in deep learning by fourier analysis’, *arXiv preprint arXiv:1808.04295* .
- Xu, Z.-Q. J., Zhang, Y., Luo, T., Xiao, Y. & Ma, Z. (2019), ‘Frequency principle: Fourier analysis sheds light on deep neural networks’, *arXiv preprint arXiv:1901.06523* .
- Xu, Z.-Q. J., Zhang, Y. & Xiao, Y. (2018), ‘Training behavior of deep neural network in frequency domain’, *arXiv preprint arXiv:1807.01251* .
- Zhang, Y., Xu, Z.-Q. J., Luo, T. & Ma, Z. (2019), ‘Explicitizing an implicit bias of the frequency principle in two-layer neural networks’, *arXiv preprint arXiv:1905.10264* .